# A Wireless Reflectance Pulse Oximeter With Digital Baseline Control for Unfiltered Photoplethysmograms

Kejia Li, *Student Member, IEEE*, and Steve Warren, *Member, IEEE*

***Abstract*—Pulse oximeters are central to the move toward wearable health monitoring devices and medical electronics either hosted by, e.g., smart phones or physically embedded in their design. This paper presents a small, low-cost pulse oximeter design appropriate for wearable and surface-based applications that also produces quality, unfiltered photo-plethysmograms (PPGs) ideal for emerging diagnostic algorithms. The design's "filter-free" embodiment, which employs only digital baseline subtraction as a signal compensation mechanism, distinguishes it from conventional pulse oximeters that incorporate filters for signal extraction and noise reduction. This results in high-fidelity PPGs with thousands of peak-to-peak digitization levels that are sampled at 240 Hz to avoid noise aliasing. Electronic feedback controls make these PPGs more resilient in the face of environmental changes (e.g., the device can operate in full room light), and data stream in real time across either a ZigBee wireless link or a wired USB connection to a host. On-board flash memory is available for store-and-forward applications. This sensor has demonstrated an ability to gather high-integrity data at fingertip, wrist, earlobe, palm, and temple locations from a group of 48 subjects (20 to 64 years old).**

***Index Terms*—Filter-free, high-fidelity photoplethysmogram, low cost, pulse oximeter, reflectance sensor, surface biosensor, wearable, wireless.**

## I. Introduction

HEALTH problems such as cardiovascular disease, hypertension, diabetes, and congestive heart failure continue to plague society [1]. These conditions are primary drivers for the development of wearable and mobile health monitoring technologies that offer the potential to (a) increase the quality of life for individuals that already suffer from these health conditions and (b) prevent or mitigate the onset of disease in those that are at risk to acquire these health issues [2]. Of the array of medical devices that can be brought to bear for wearable/mobile applications that address these diseases, pulse oximeters offer significant relative promise because they provide two clinically relevant health parameters [heart rate (HR) and blood oxygen saturation ($SpO_2$)], they do not require electrical contact to tissue, and they can operate at very low power [3], [4]. Additionally, the pulsatile plethysmographic data offered by this light-based sensing technique (which are usually discarded by commercial pulse oximeters after being used to calculate the parameters for the front panel display) can help to ascertain hemodynamic information that is well-suited for the assessment of the disease states listed above [5]–[8]. This information includes blood pressure [9], [10], arterial compliance [6], [11], [12], pulse wave velocity (PWV) [2], [13], stroke volume (and therefore cardiac output) [14], and other vascular parameters [7], [8], [15], [16]. Other relevant quantities include respiration rate [17], [18], patient motion [16], and even patient authentication [19]–[21].

However, low-cost pulse oximeter designs are unavailable that provide (a) quality, unfiltered PPGs ideally suitable for research and education toward the realization of new PPG diagnostics and (b) positional flexibility suitable for mobile and surface-based applications. While PPGs are often accessible from commercial desktop units via serial ports, these data have been filtered in proprietary ways to stabilize HR and $SpO_2$ calculations. Further, due to their clinical prevalence, pulse oximetry and PPG analysis deserve coverage in biomedical instrumentation laboratories offered in secondary education curricula, yet low-cost pulse oximeters that provide reasonable-quality PPGs are not a staple in off-the-shelf educational kits.

Regarding ambulatory pulse oximeters, several types of wearable designs exist. Some of these use ring form factors, and others use finger clips. These designs use predominantly transmission-mode sensors. For broader use with wrist watches, head bands, socks, sensor 'Band Aids', and other wearable platforms that are unobtrusive and well suited for mobility, it makes sense to consider reflectance-mode layouts. This is especially true when one contemplates the immense potential of 'surface biosensors' (SBs): medical sensors embedded in the surface of everyday consumer electronics such as hand-held personal device assistants (PDAs), cell phones, smart phones, tablet PCs, head-mounted displays, etc. In this paradigm, physiological sensors will be accessible and signals will be easy to obtain, as human factors considerations for the overall product design will drive ease of use for the integrated biosensors. Additionally, each SB will utilize its host device's processor, memory, display, and wireless communication resources to provide user services typically unavailable in wearable platforms [22]. E.g., consider a reflectance pulse oximeter embedded on the back side of a cell phone alongside a built-in camera. As the user holds their finger against the reflectance sensor, these data will be processed by the microprocessor in the cell phone, and the LCD screen will display the signals and parameters.

In this domain, a reflectance sensor can employ a single small photodiode [23] as in most transmittance sensors. However,

Manuscript received December 03, 2010; revised April 24, 2011 and July 18, 2011; accepted August 15, 2011. Date of publication November 04, 2011; date of current version May 22, 2012. This work was supported in part by the National Science Foundation under Grants BES-0093916, BES-0440183, and CNS-0551626, and by the Kansas State University Targeted Excellence Program. Opinions, findings, conclusions, or recommendations expressed in this material are those of the author(s) and do not necessarily reflect the views of the NSF. This paper was recommended by Associate Editor E. Jovanov.

The authors are with the Department of Electrical and Computer Engineering, Kansas State University, Manhattan, KS 66506 USA (e-mail: kejiali@ksu.edu; swarren@ksu.edu).

Color versions of one or more of the figures in this paper are available online at http://ieeexplore.ieee.org.

Digital Object Identifier 10.1109/TBCAS.2011.2167717

tissue is highly forward scattering, so the relative number of remitted photons detected in reflectance mode is low, yielding lower quality PPGs [5]. Improved sensor configurations are therefore often adopted to better acquire the radial reflectance profile, including a ring-shaped photodiode design [24], [25], a photodiode array around the central LEDs [26], and conversely an LED array around a central photodiode [27]. These designs generally employ cascaded high pass and low pass filters to extract the PPGs [28]. Such analog filters inevitably alter and even distort the signals of interest. These alterations are visibly obvious in some papers, and cycle-to-cycle inconsistencies can be significant. For this reason, a filter-free design is desirable. Finally, in a low-cost wearable sensor with a limited voltage range (e.g., [0, 3.3] V if battery powered) and a low-precision analog-to-digital converter (e.g., 8 to 12 bits), maintaining a sensible vertical resolution, number of digitization levels, and sampling frequency for a PPG can be difficult without flexible baseline subtraction and PPG amplification strategies.

In summary, the desire to extract additional physiological information from PPGs acquired with reflectance-mode sensors imposes design constraints with respect to signal quality. This paper presents the design of a low-cost, wireless, reflectance-mode pulse oximeter suitable for these needs. It is initially housed on the surface of a printed circuit board but can be easily migrated to other surface-based applications. Here, a unique filter-free circuit (that digitally extracts the PPG waveform) and a two-stage, feedback-loop-driven control system enable the acquisition of unfiltered PPGs with $2^{12} = 4096$ levels of precision from varied body locations. An optimized LED/detector configuration promotes surface use, and the device signal quality and cost enhance its potential for integration into SB-based consumer devices.

## II. Methods

This section presents a design for a filter-free, reflectance pulse oximeter that combines many desirable features into a single platform. Implementation hardware is unspecified here; board-level components are detailed in Section III. Device Prototype.

### A. Requirements and Device Layout

The design requirements are outlined in Table I. Signal requirements include quality, unfiltered PPGs whose baselines are digitally removed, consistent with the discussion in Section I. Introduction. The high sampling rate ensures that (a) primary signal and noise components are adequately sampled without aliasing and (b) secondary noise harmonics, e.g., 120 Hz up to several kHz from fluorescent lighting, are not aliased on top of the signal components of interest.

Regarding sensor requirements, the photodetectors are ideally distributed radially around the central excitation LEDs to maximize the number of photons collected. Further, an LED/detector separation of 3 to 5 mm is appropriate at these wavelengths, as it maximizes the AC/DC ratio for each sensor channel, as verified experimentally [26], [29] and with Monte Carlo simulations [21]. In other words, reflectance photons that contain DC information from shallow, poorly perfused epidermal layers reflect near the central excitation LEDs and are undetected. Photons collected at greater radial distances are more likely to have traveled deeper into blood-perfused tissue and contain a greater percentage of AC data. Given the increased sensing area in a large-area detector, the control circuitry must easily compensate for baseline changes due to ambient light, tissue perfusion, respiration depth, etc.

TABLE I
Wireless Reflectance Pulse Oximeter Design Requirements

| *Category* | *Requirements* |
|---|---|
| **Signal** | |
| Integrity | Unfiltered data with an optimal SNR |
| Precision | Thousands of peak-to-peak digitization levels |
| Sampling frequency | ≥ 240 Hz to minimize PPG/noise aliasing |
| Baseline subtraction | Digital and filter-free |
| Data availability | Full access to all pulsatile/baseline data |
| **Sensor** | |
| LED/detector geometry | Radial arrangement, large area, and 3-5 mm source/detector separation |
| Ambient light operation | Adjustable gain and reference baseline |
| **Functionality** | |
| Communication | Wireless (10 m range) and USB |
| Local storage | Onboard flash memory |
| Battery | USB-rechargeable; Multi-day lifetime |
| Client Software | Visualization and control panel |
| **Application** | |
| Measurement sites | Multiple body locations; Various vascular profiles and perfusion levels |
| Wearability | Low-profile reflectance layout adaptable for wearable and SB applications |
| Cost | Low (<$100) |

Fig. 1 shows the block diagram for the pulse oximeter circuitry; a brief description was also included in [30]. The LED, sensor array, and operational amplifier (OPA) circuitry are coordinated by a Jennic JN5139 microcontroller. The intensity and timing of the bi-color LED are controlled by a digital-to-analog converter (DAC) and digital input/output ports (DIOs), respectively. A signal from the sensor array (four photodiodes surrounding the central bi-color LED) is first buffered and then fed to a differential OPA circuit. The buffered signal, designated here as the first-stage PPG signal (entire AC + DC contribution), is sampled by an analog-to-digital converter (ADC). Another ADC collects the second-stage PPG signal (the AC portion only) from the output of the differential OPA circuit that has a positive input from another microcontroller DAC.

No filters are used in the signal acquisition process, whose elements will be introduced in *Part C. Closed-Loop System*. The battery (unstable power source) is isolated from the PPG excitation and collection circuitry, since it is powered by the microcontroller's analog peripheral regulator (APR). Normally, the pulse oximeter uses a wireless link to communicate with a receiver on a PC, and data are stored on the PC through a MATLAB graphical user interface (GUI). A mini-USB connection can provide a wired interface to the PC while the battery is recharged. If neither the wireless link nor the USB connection is available, sampled data will be temporarily stored on the flash memory module (e.g., for store-and-forward applications).

### B. AC Extraction and Drift Resistance

The first-stage PPG is characterized by a large DC portion and a small AC portion, as in Fig. 2. The goal is to extract the

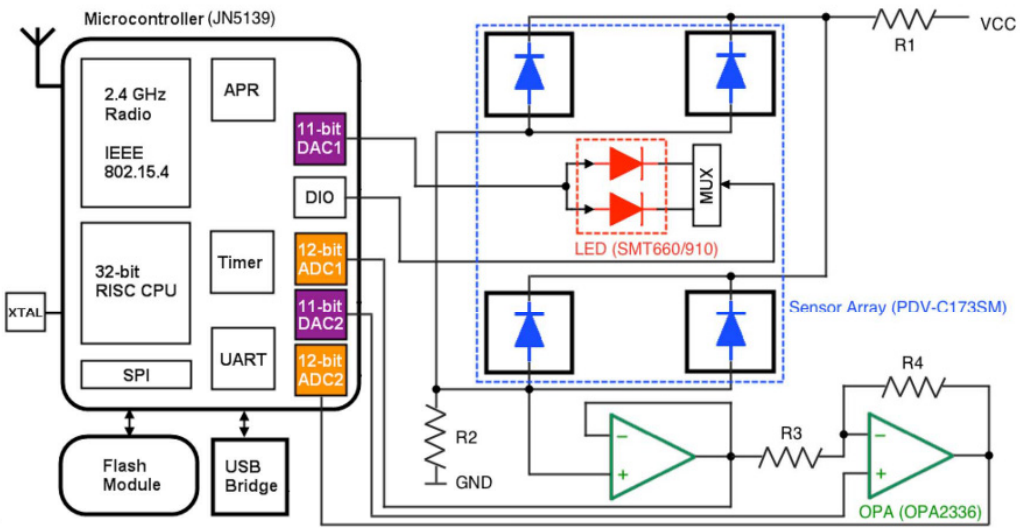


Fig. 1. Circuit-level system layout. Coordinated by the microcontroller, signal baselines are digitally extracted as an alternative to conventional filtering.

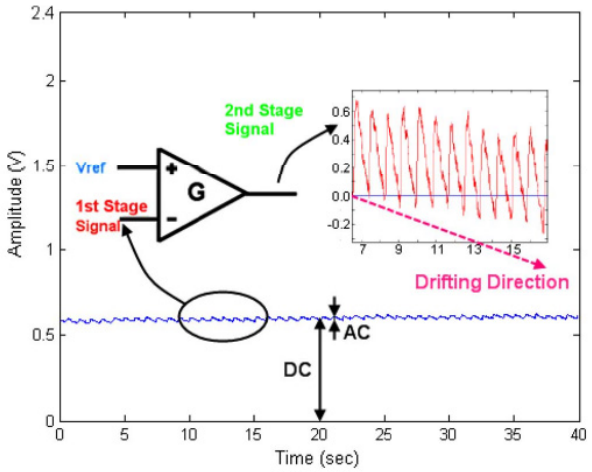


Fig. 2. A differential amplifier with gain $G$ compares the first-stage PPG ($S_1$) to a DC reference voltage to obtain the second-stage PPG ($S_2$).

second-stage AC signal by eliminating the DC component. (In many systems, a high pass filter extracts the AC signal.) If the DC portion instead remains, then obtaining hundreds to thousands of digitization levels in the AC portion over its small voltage range requires an ADC of very high precision (e.g., 16-bit), which is inappropriate for a low-cost, low-power-consumption device. This extraction, or DC removal, process is executed by the OPA unit. Its role is expressed as

$$S_2 = G \times (V_{ref} - S_1) \tag{1}$$

where $S_1$ and $S_2$ are the first-stage and second-stage signals, respectively, $G$ is the gain of the OPA, and $V_{ref}$ is a user-defined reference voltage that functionally equates to the DC signal level. To show an upward-oriented PPG peak during systole as with a blood pressure curve, $V_{ref}$ is connected to the positive pin of the OPA, effectively inverting the AC signal amplitude prior to digitization.

$S_1$ is naturally unstable, as both its AC and DC levels are influenced by changes in intrinsic blood flow, extrinsic motion, respiration, background light, etc. These factors cause drifting in $S_2$. The input voltage range, or digitization range, of the 12-bit ADC is set to [0, 2.4] V, so one digitization level is $2.4\ \mathrm{V}/4095\ \mathrm{levels} = 0.586\ \mathrm{mV}$. For example, given a gain $G = 30$ and a constant $V_{ref}$, one digitization-level increment in the DC signal results in a decrement of 30 digitization levels in $S_2$ according to (1). As in Fig. 2, $S_2$ may drift 0.3 V (512 digital levels) in 10 seconds, which is unacceptable because the signal will eventually clip at the lower bound of the sampling range, and clipped data mean signal corruption. To address this issue, (1) implies that one can adjust one or more elements on the right side to adjust the value of $S_2$ on the left. In this effort, a $V_{ref}$ adjustment is employed to resist $S_2$ drifting, since $V_{ref}$ is an output of the DAC and can be easily updated. $V_{ref}$ is defined as

$$V_{ref} = MA(t) + V_+ \tag{2}$$

where $MA(t)$, the estimator of the DC component, $V_{DC}$, is a $W$-point (e.g., $W = 256$) moving average of the first-stage signal over the time interval that ends at $t$. $V_+$ (the adjustable term) is added to $MA(t)$ to ensure that $V_{ref}$ makes $S_2$ in (1) positive.

$V_{ref}$ usually varies slowly (several seconds per digitization level change, in an environment with minimal motion and ambient noise), and the $V_{ref}$ adjustment leads to a discontinuity in $S_2$. Hence, the $V_{ref}$ data must also be transmitted or stored along with the digitized second-stage data in order to restore the original PPGs, a process called "compensation."

Fig. 3 shows a data set from the palm. Collected data are compensated to remove discontinuities caused by $V_{ref}$ jumps, or immediate value changes, in the pulsatile waveform using

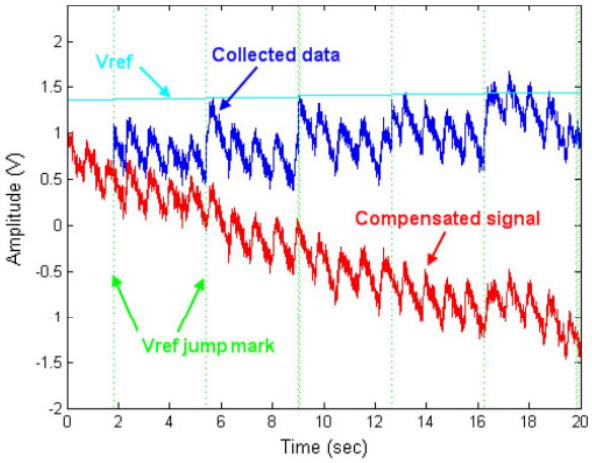


Fig. 3. Palm PPG data before (blue) and after (red) compensation.

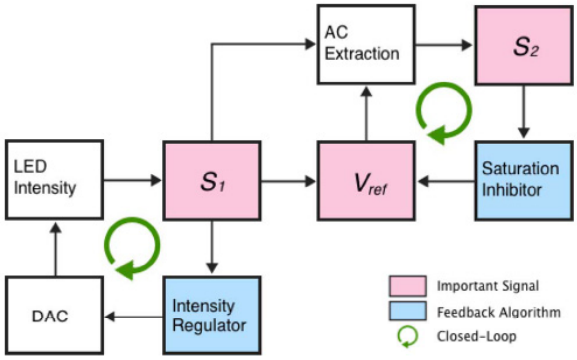


Fig. 4. Pulse oximeter control flow that illustrates how the first-stage PPG ($S_1$) can be used to create the second-stage PPG ($S_2$), where both signals provide feedback to stabilize the acquisition process.

the following method. Inserting $V_{ref}$ from (2) into (1) and then rearranging the result isolates the first-stage signal, $S_1$

$$S_1 = MA(t) + V_+ - \frac{S_2}{G}. \tag{3}$$

The compensated second-stage signal, $\hat{S}_2$, can be represented as

$$\hat{S}_2 = G \times (V_{DC} + V_+ - S_1) \tag{4}$$

where $V_+$ is added to $V_{DC}$ to ensure a positive $\hat{S}_2$. Substituting (3) into (4) yields

$$\hat{S}_2 = S_2 - G \times (MA(t) - V_{DC}). \tag{5}$$

Typically, $V_{DC}$ is an unknown constant, but it is sensible to initially set $V_{DC} = MA(t_0)$ at time $t_0$ and define $V_{jump} = MA(t) - MA(t_0)$ at time $t$ $(t > t_0)$ so that (5) becomes

$$\hat{S}_2 = S_2 - G \times V_{jump}. \tag{6}$$

With this method, each PPG can be restored as long as the second-stage signal is unsaturated. The $V_{ref}$ adjustment effectively resists first-stage-signal drifting. For example, in Fig. 3, the compensated signal drifts below 0 V after 6 seconds. If no $V_{ref}$ adjustment occurs, the subsequent signal is sampled as 0 V. To calculate blood oxygen saturation, $V_{ref}$ is usually considered equal to $V_{DC}$.

### C. Closed-Loop System

The $V_{ref}$ adjustment mechanism not only helps to realize the AC extraction task; it also results in resilience in the PPG signal. In the control system, as illustrated in Fig. 4, two closed loops provide stability for the whole data acquisition process. The closed loop in the lower left maintains the $S_1$ value in a predetermined range, which is set by the Intensity Regulator that controls the led intensity via a DAC. The physical function of this control loop is to maintain the number of reflected photons at an optimal level within the active range of the photodiode, independent of a subject's vascular and perfusion profiles [30]. The closed loop in the upper right prevents $S_2$ from saturation, since the compensation method described in (6) requires an unsaturated second-stage signal. Upon detecting saturation onset, the Saturation Inhibitor adjusts the $V_+$ component of $V_{ref}$, which leads to a corresponding change in $S_2$ according to (1).

To maintain signal quality, the Intensity Regulator sensitivity should be minimized. When the regulator affects changes in LED excitation level, the influence on the first-stage signal converted by the photodiode sensor array will be hard to predict because the blood-perfused tissue between the LED and the sensor is an unknown system. Conversely, the sensitivity of the Saturation Inhibitor should be set high to ensure a rapid response to signal drift. Since this adjustment only influences $V_{ref}$, the native PPG is uncontaminated, and the second-stage signal can be adjusted using (6).

In a controlled scenario, ambient noise variations can be ignored. If the desired signal intensity increases as the LED intensity increases, the signal-to-noise ratio (SNR) will improve. However, this implies a saturation risk due to a second-stage signal with too large of a magnitude within a fixed digitization range, in spite of the aforementioned drift-resistant method. Additionally, a more intense LED consumes more power. So, an optimized intensity level should be empirically predetermined as an Intensity Regulator reference.

### D. Removable Noise

In the U.S.A, ambient light often includes a 60 Hz component and the associated harmonic noise, e.g., 120 Hz flicker from full-wave-rectified fluorescent room lights plus higher-frequency harmonics. Most physiological information in a PPG resides in the range of 0–20 Hz. From the Nyquist-Shannon sampling theorem, the lowest sampling frequency, $f_s$, should then be 40 Hz, but to prevent ambient noise aliasing, sampling frequencies of at least 240 Hz are needed.

Fig. 5 depicts the magnitude spectrum of a PPG containing ambient noise. The heart rate component is 1.329 Hz, and its harmonics dominate in the frequency band below 20 Hz. At greater frequencies, noise is apparent at 60.02 Hz, 84.43 Hz (unclear source), and 119.9 Hz. Most of this noise is removable

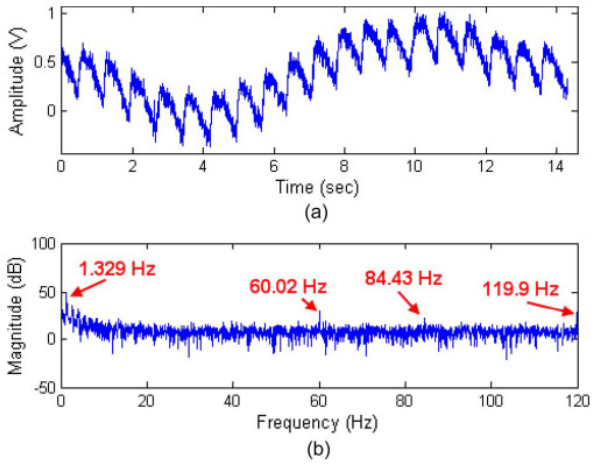


Fig. 5. An example of removable noise. (a) Compensated PPG corrupted by ambient noise. (b) Frequency spectrum of these data sampled at 240 Hz.

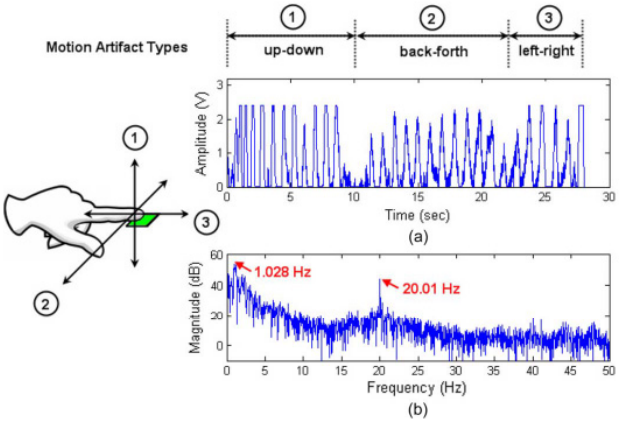


Fig. 6. (a) PPG severely corrupted by hand motion along three axes. (b) Frequency spectrum of the 28 seconds of data sampled at 100 Hz.

by post-processing as long as the sampling frequency is high enough that these noise components do not alias into the frequency range of the signal components of interest. Note that the raw signal exhibits a low SNR compared to PPGs from pulse oximeters that employ filters, but all signal components are intact and many can be removed to create a high SNR (see Fig. 12).

### *E. Motion Artifact*

Motion artifact is an issue for a pulse oximeter, especially in reflectance mode [5]. Existing literature focuses on signal processing to reduce motion artifact and restore PPGs [31]. Most methods assume that enough information exists in the corrupted signal for PPG recovery. However, if motion is severe, saturation occurs frequently and lasts for some time, leading to data loss. With this in mind, this development considered motion artifact to be a type of signal drift that can be partially addressed with a drift-resistant method ($V_{ref}$ adjustment); the design does not address motion extraction.

Motion artifact can be classified into two categories: slight and severe. Fig. 6 demonstrates the severe condition characterized by three axes of hand motion, where the sensor is taped to the finger. Movements are within a 10 cm range and occur at a rate of ~1 Hz. The PPG is severely corrupted (the fundamental frequency is 1.028 Hz), and it is clipped at the upper and lower bounds of the digitization range; many AC segments are lost and unrecoverable.

The slight condition refers to, e.g., slow body movements, where a PPG retains its general shape but contains spurious components relative to a still condition. To counteract this type of artifact, the shift-resistant method is promising and relies on the setting of an optimal assignment rate and window width for $V_{ref}$ adjustment. The DAC assigns the $V_{ref}$ value to the positive amplifier pin, and that voltage remains constant until the next $V_{ref}$ assignment to the DAC. The window size of the moving average filter (the DC estimation time delay, or count) and the rate of assigning $V_{ref}$ to the DAC (not the rate of $V_{ref}$ variation) influence the second-stage signal. An extreme case occurs when the window size $W = 1$ data point and the rate of assigning $V_{ref}$ to the DAC is $A = f_s$: motion will never influence

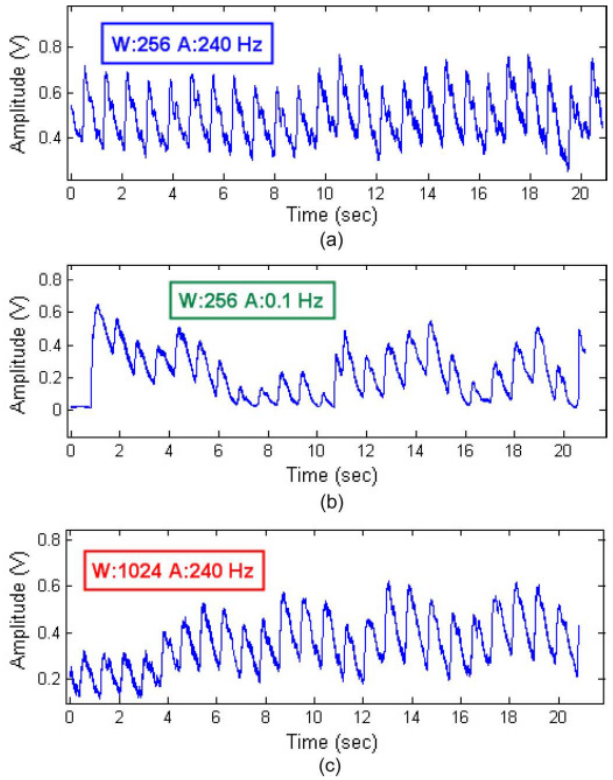


Fig. 7. Three uncompensated PPGs acquired at $f_s = 240$ Hz under similar slight-motion conditions but with different parameter pairs $(W, A)$.

the signal since $MA(t) \equiv S_1$ and consequently $S_2 = G \times V_+$ according to (1) and (2).

As an illustration of slight motion response, Fig. 7 shows three experimental records acquired under similar conditions (exaggerated deep respiration activity), where a different moving-average window width, $W$, and $V_{ref}$ assignment rate, $A$, are employed in each case. Only subplot (a) offers a reasonable representation of the PPG. A lower assignment rate (b) or wider window (c) causes the signal to drift severely, and some

DOCKET ALARM

# Explore Litigation Insights

Docket Alarm provides insights to develop a more informed litigation strategy and the peace of mind of knowing you're on top of things.

## Real-Time Litigation Alerts

Keep your litigation team up-to-date with **real-time alerts** and advanced team management tools built for the enterprise, all while greatly reducing PACER spend.

Our comprehensive service means we can handle Federal, State, and Administrative courts across the country.

## Advanced Docket Research

With over 230 million records, Docket Alarm's cloud-native docket research platform finds what other services can't. Coverage includes Federal, State, plus PTAB, TTAB, ITC and NLRB decisions, all in one place.

Identify arguments that have been successful in the past with full text, pinpoint searching. Link to case law cited within any court document via Fastcase.

## Analytics At Your Fingertips

Learn what happened the last time a particular judge, opposing counsel or company faced cases similar to yours.

Advanced out-of-the-box PTAB and TTAB analytics are always at your fingertips.

## API

Docket Alarm offers a powerful API (application programming interface) to developers that want to integrate case filings into their apps.

**LAW FIRMS**
Build custom dashboards for your attorneys and clients with live data direct from the court.

Automate many repetitive legal tasks like conflict checks, document management, and marketing.

**FINANCIAL INSTITUTIONS**
Litigation and bankruptcy checks for companies and debtors.

**E-DISCOVERY AND LEGAL VENDORS**
Sync your system to PACER to automate legal marketing.